Analysis of Two-Dimensional Viscous Flow over Cylinders in Unsteady Motion

Mohammad E. Taslim* and Robert B. Kinney†
The University of Arizona, Tucson, Arizona
and
Michael A. Paolino‡
U.S. Military Academy, West Point, New York

The two-dimensional, viscous flow around elliptic cylinders undergoing prescribed rotary and translational motions is analyzed. The fluid is taken to be incompressible and initially at rest. Departing from conventional numerical formulations, the body is replaced by fluid which has a rigid motion exactly the same as the actual solid body. This is achieved by placing a uniform vorticity field within the body (equal to twice the instantaneous angular velocity), and bound vorticity on the body surface in the form of a vortex sheet. The latter distribution is governed by an integral equation. The solution is made unique by the principle of conservation of total vorticity. This depends on the instantaneous angular velocity of the body, the new ingredient to this analysis. The free vorticity in the outer flowfield is governed by the usual vorticity transport equation, which is solved numerically. The velocity field is determined by the velocity induction law. Transient flow results are presented for 1) an elliptic cylinder started impulsively from rest with constant angular velocity, and 2) a pitching elliptic cylinder moving with constant translational velocity. Results for case 1 are compared with those from a previous numerical analysis. Previous results for case 2 are not known. Predictions for the drag, lift, and moment coefficients are given over two complete cycles of oscillation.

Nomenclature

a = semimajor axis of the elliptic cylinder, radius of circular cylinder
b = semiminor axis of the elliptic cylinder
c = $[1-(b/a)^2]^{1/2}$, nondimensional focal distance of the ellipse
$(C_D)_F$ = $D_F/\rho\hat{U}^2 a$, friction drag coefficient
$(C_D)_P$ = $D_P/\rho\hat{U}^2 a$, pressure drag coefficient
$(C_L)_F$ = $L_F/\rho\hat{U}^2 a$, friction lift coefficient
$(C_L)_P$ = $L_P/\rho\hat{U}^2 a$, pressure lift coefficient
$(C_M)_F$ = $M_F/\rho\hat{U}^2 a^2$, moment coefficient due to friction
$(C_M)_P$ = $M_P/\rho\hat{U}^2 a^2$, moment coefficient due to pressure
D_F, D_P = friction and pressure drag per unit span
$\hat{e}_\xi, \hat{e}_\eta$ = unit vectors in ξ and η directions, respectively
h = $[1-(b/a)^2]^{1/2}\,[\sinh^2\xi+\sin^2\eta]^{1/2}$, nondimensional metric coefficients in elliptical coordinate system
$\hat{i},\hat{j},\hat{k}$ = unit vectors in x, y, and z directions
M_F, M_P = pitching moments per unit span due to friction and pressure, respectively; moment is positive in counter-clockwise direction
P = nondimensional pressure
q_ξ, q_η = nondimensional fluid velocity components in ξ and η directions
r_{ab} = $r_b - r_a$
Re = $\hat{U}a/\nu$, Reynolds number
t = nondimensional time
$\hat{U}$ = characteristic velocity of the cylinder (dimensional)
U_b, V_b = nondimensional translational velocity components of the body in the x and y directions, respectively
$\dot{U}_b, \dot{V}_b$ = nondimensional rectilinear acceleration components of the body in the x and y directions, respectively
u_x, u_y = nondimensional velocity components in the x and y directions induced by the internal vorticity, respectively
u_ξ, u_η = nondimensional fluid velocity components relative to a stationary frame in ξ and η directions, respectively
x, y = nondimensional Cartesian coordinates attached to the body
X, Y = stationary Cartesian coordinate system
α = angle between the x axis and the line of action of the velocity vector of the body, as shown in Fig. 1
β = angle between the stationary coordinate system and that attached to the body, as shown in Fig. 1
γ = nondimensional bound vorticity; $\hat{\gamma}=\gamma h$
η, ξ = elliptic coordinates
ν = kinematic viscosity
ω_f = nondimensional free vorticity
Ω = nondimensional angular velocity of the body
Ω^* = dimensional angular velocity
$\dot{\Omega}$ = nondimensional angular acceleration of the body

Received July 8, 1982; revision received May 24, 1983.

*Assistant Professor, Mechanical Engineering Department, Northeastern University, Boston, Mass.
†Professor, Aerospace and Mechanical Engineering Department. Associate Fellow AIAA.
‡Associate Professor and Colonel, Department of Mechanics.

Introduction

THE computation of unsteady external flows in two dimensions has occupied the attention of researchers for more than two decades. The most thoroughly studied flows have been those about circular and elliptic cylinders; and, most frequently, the flow is considered to be started from rest impulsively. That is, the cylinder is assumed to be fixed, and at some instant in time, the fluid is set into motion with some

uniform and constant translational velocity. This is dynamically and kinematically equivalent to setting the body into motion impulsively in an initially stationary fluid, provided the flowfield is viewed in a coordinate system moving with the cylinder.

Numerical studies in which the body has a time-varying motion or the external flow varies with time are relatively few in number. Mehta[1] has used the vorticity streamfunction approach to study flow past an airfoil undergoing pitching oscillations in a uniform stream. Results have been presented for Reynolds numbers of 5000 and 10,000. Wu[2] has applied his integro-differential formulation also to flow past an oscillating airfoil for a Reynolds number of 1000. The case of a stationary airfoil submerged in a stream with constant speed but time-varying flow angle has been analyzed by Kinney.[3] The largest Reynolds number considered was 10,000. More recently, the flow development past a thin elliptic cylinder set into motion with a translational velocity which varies linearly with time has been calculated by Lugt and Haussling.[4] Results for a Reynolds number of 200 were obtained using the vorticity streamfunction formulation. In each of these works, the analyses have been specialized to the particular motions under investigation.

In the present study, we enlarge upon these earlier works and consider the most general class of two-dimensional body motions. The body is taken to be a cylinder which is initially at rest in a stationary fluid. At some instant in time the body is set into motion with translational velocity and rotational speed which are specified functions of time. All plane motions can be represented in this manner, and a unified formulation is given which includes as special cases the body motions considered in the above cited references. The method is applied to elliptic cylinders undergoing various kinds of rotational and translational motions.

Basis of Theoretical Approach

The basic approach used by Kinney and Cielak[5] is generalized and extended to include the present class of two-dimensional body motions, namely, those with angular velocities. As before, the actual solid body is considered to be replaced by fluid with suitable vorticity distributions over its surface (bound vorticity) and interior (body vorticity). It is this latter distribution which represents the new ingredient to the analysis. These two vorticity distributions must be so constituted that the entire replacement fluid follows the prescribed rigid body motion. In general, there will also be free vorticity in the fluid exterior to the body. This constitutes the boundary-layer and wake regions.

It is well known[6] from potential-flow theory that the body interior must be filled with vorticity which is uniform and equal in magnitude to twice the instantaneous angular velocity of the body [i.e., $2\Omega(t)$]. The bound vorticity is governed by an integral equation, the solution of which is nonunique. The ambiguity to the solution must be removed, and this is done by enforcing the law for the conservation of total vorticity. This law must now include the effects of the body vorticity, the ingredient previously absent. Once the bound vorticity on the surface is determined, the enforcement of the tangential adherence condition allows the local production and diffusion of free vorticity from the surface into the fluid to be specified. This is in keeping with the previous philosophy. The key step, then, is the determination of the bound vorticity distribution on the surface.

Wu[7] has reviewed the mathematical foundations for this approach, which are quite classical in nature. The need to enforce an integral law for the conservation of total vorticity is emphasized, but the method of doing so is not mentioned. The importance of this law cannot be overstressed. As remarked earlier and shown later, it provides the closure for the unique determination of the bound vorticity on the surface of the body. Also, it ensures that the pressure distribution on the surface of the body is single valued.

Simply stated, the law for the conservation of total vorticity requires that the rate at which net vorticity is produced at the solid surface must equal the negative of the instantaneous time rate of change of the total vorticity of the replacement fluid within the body. However, it has never been made clear how this integral law should be incorporated into the surface boundary conditions which are to be enforced in the numerical calculations. The previous work of Wu[7] is the only one known to the authors that attempts to address this question. Most investigators simply ignore it and proceed to determine the fluid vorticity at points on the body surface which locally reduces the slip velocity to zero. Wu, on the other hand, determines the surface vorticity of the fluid from the bound vorticity, which is calculated from an integral equation. He divides the local value of the bound vorticity by a suitable incremental distance from the wall in order to obtain the fluid vorticity at the wall. This has the effect of spreading the bound vorticity of the surface over a sheet of fluid with finite thickness. Although not explicity stated, the diffusion of vorticity into the fluid, which afterall is the relevant quantity under consideration, is presumably evaluated using a finite difference formula which involves the vorticity at the wall and at some adjacent data points in the fluid. Unfortunately, if this is then used to determine the total net vorticity which is cast off into the fluid from the entire body, there is no guarantee that it will equal the instantaneous time rate of change of total vorticity of the replacement fluid within the body, as required by the conservation law. This is because the bound vorticity is itself ambiguous, since it cannot be determined uniquely from its governing integral equation alone. Further complications arise because the vorticity values from within the fluid are needed to form this diffusion term, and these are determined by earlier events and not just those occurring instantaneously.

The approach used here avoids this difficulty entirely and leads to a completely consistent and unambiguous formulation. This is possible because the surface diffusion of vorticity (more correctly, the time-integral of it) is determined directly in the analysis rather than the surface value of vorticity. It is this feature which has most fundamentally separated the integral formulations of Wu and Kinney.

Analysis

We consider here only bodies with cross sections which are elliptical or circular. Therefore, it is convenient to adopt the elliptical coordinate system for the external flow description.

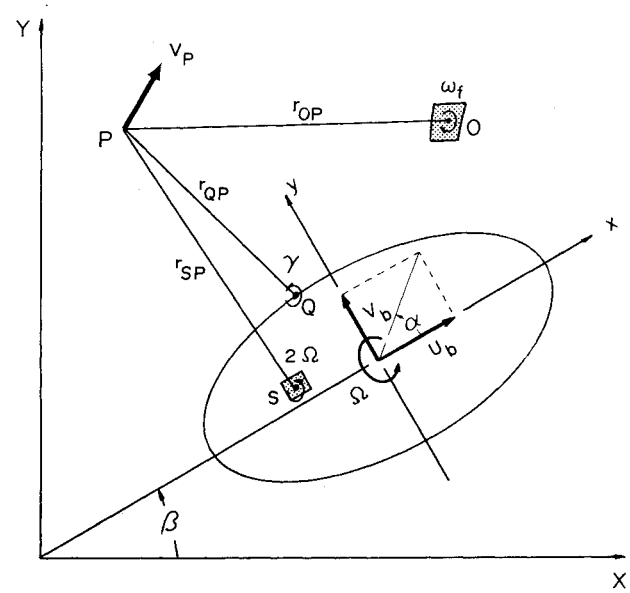

Fig. 1 Diagram of coordinate system showing contributions of different vorticities to the induced velocity.

The surface of the body is given by $\xi = \text{const} = \xi_0$. The η coordinate varies from 0 to 2π around the body in a counter-clockwise direction, the point $\eta = 0$ being taken on the positive x axis of a Cartesian coordinate system.

The formal coordinate transformation is given by $x + iy = c \cosh(\xi + i\eta)$. Let a and b denote, respectively, the semimajor and semiminor axes of the body. Then, $b/a = \tanh \xi_0$ is the aspect ratio. All lengths are scaled relative to a, such that $c = 1/\cosh \xi_0 = (1 - b^2/a^2)^{1/2}$.

The detailed development of the working form of the governing equations, particularly those used in the numerical evaluations, is too lengthy to give here. This is well documented in the dissertation[8] on which this paper is based. Therefore, only the basic ideas and highlights will be given.

Governing Equations

The velocity vector at any point P in the flow is determined by the law of induced velocities. Here we consider three separate vorticity distributions, as shown in Fig. 1. These are the free vorticity of the fluid ω_f, the bound vorticity of the surface γ, and the body vorticity interior to the cylinder 2Ω. The velocity vector is given by

$$V_P = \frac{1}{2\pi}\int_{\xi_0}^{\infty}\int_0^{2\pi}\left[\frac{\omega_f \hat{k}\times r_{OP}}{r_{OP}^2}\right]h^2(\xi,\eta)\,d\eta\,d\xi + \frac{\Omega}{\pi}\int_0^{\xi_0}\int_0^{2\pi}\left[\frac{\hat{k}\times r_{SP}}{r_{SP}^2}\right]h^2(\xi,\eta)\,d\eta\,d\xi + \frac{1}{2\pi}\int_0^{2\pi}\left[\frac{\gamma\hat{k}\times r_{QP}}{r_{QP}^2}\right]h(\xi_0,\eta)\,d\eta \tag{1}$$

The points O, S, and Q give the locations of the three vorticity distributions, and the vectors r_{OP}, r_{SP}, and r_{QP} are directed from these points toward P. It easily is verified that only the first integral in Eq. (1) contributes to the rotational part of the velocity field. The other contributions are purely potential in nature.

The quantity h is the metric coefficient, given in dimensionless form by $h = [1 - (b/a)^2]^{1/2}\,[\sinh^2\xi + \sin^2\eta]^{1/2}$. The velocity is made dimensionless with $\hat{U}$, where $\hat{U}$ is a yet to be prescribed characteristic velocity of the system.

The velocity V_P is the absolute velocity in an inertial coordinate system fixed relative to the external fluid, which is at rest at infinity. At any instant in time, we may locate the field points in the fluid through our elliptic coordinate system, which is fixed to the body. This coordinate system is noninertial, however, since it is subjected to the prescribed accelerations of the body.

The free vorticity ω_f is governed by the following nondimensional transport equation.

$$\frac{\partial}{\partial t}\omega_f + \frac{1}{h^2}\frac{\partial}{\partial \xi}(hq_\xi\omega_f) + \frac{1}{h^2}\frac{\partial}{\partial \eta}(hq_\eta\omega_f) = \frac{(1/Re)}{h^2}\left(\frac{\partial^2\omega_f}{\partial\xi^2} + \frac{\partial^2\omega_f}{\partial\eta^2}\right) \tag{2}$$

The vorticity and time variables are rendered nondimensional using a and $\hat{U}$, and $Re = a\hat{U}/\nu$.

Note that ω_f is the absolute vorticity (i.e., curl of $\bar{V}$). It is convected with the relative velocities, q_ξ and q_η, which can be obtained through kinematical considerations. Let u_ξ and u_η denote the components of absolute velocity as obtained from Eq. (1). If the body moves with velocity components as shown in Fig. 1, then one can write

$$V = u_\xi\hat{e}_\xi + u_\eta\hat{e}_\eta = q_\xi\hat{e}_\xi + q_\eta\hat{e}_\eta + (U_b - y\Omega)\hat{\imath} + (V_b + x\Omega)\hat{\jmath} \tag{3}$$

The components of q are

$$q_\xi = u_\xi - \frac{c}{h}\left[(V_b\cosh\xi\sin\eta + U_b\sinh\xi\cos\eta) + c\Omega\sin\eta\cosh\eta\right] \tag{4a}$$

$$q_\eta = u_\eta - \frac{c}{h}\left[(V_b\sinh\xi\cos\eta - U_b\cosh\xi\sin\eta) + c\Omega\sinh\xi\cosh\xi\right] \tag{4b}$$

Observe that U_b and V_b are the components of the instantaneous translational velocity of the body as resolved along the x and y axes of the body, respectively. The body rotation is about the centroid and is considered to be positive in the counter-clockwise direction, see Fig. 1.

In practice, only the η component of absolute velocity is obtained from Eq. (1). This is done most easily by first resolving the velocity vector into components along the x and y axes. Following this, the component in the η direction is obtained by forming the scalar product of $\hat{e}_\eta$ with the Cartesian velocity components and adding them. The final result is obtained by numerical integration. The actual expressions used in the evaluations will be presented in a later section which deals with the numerical formulation.

Having obtained u_η using the procedure just described, the ξ component of absolute velocity is obtained from the equation of continuity. That is,

$$u_\xi(\xi,\eta) = \frac{h(\xi_0,\eta)}{h(\xi,\eta)}u(\xi_0,\eta) - \frac{1}{h(\xi,\eta)}\frac{\partial}{\partial\eta}\int_{\xi_0}^{\xi} h(\xi',\eta)u_\eta\,d\xi' \tag{5}$$

Note that $u_\xi(\xi_0,\eta)$ is not zero since it is the velocity component of the solid surface which is in motion. This quantity can be obtained from Eq. (4a) with $q_\xi = 0$. Finally, the relative components of velocity q_ξ and q_η are obtained at points in the fluid from Eqs. (4a) and (4b).

It remains to develop the integral equation for the bound vorticity. This is obtained from Eq. (1), as specialized for the η component of velocity at P just interior to the body. At this point in space V_P is equal to the prescribed velocity of the body. This is given by Eq. (3) with $q_\xi = q_\eta = 0$. Therefore, it is known at each instant in time. Also, the free vorticity is considered known, as is $\Omega(t)$. The only unspecified quantity in Eq. (1) is γ.

The procedure for determining γ is as follows. Let $(u_n)_{\text{outer}}$ denote the velocity component tangential to the body, which is induced by the outer free vorticity of the fluid, as given by the scalar product of the first integral on the right-hand side of Eq. (1) and the unit vector $\hat{e}_\eta$. The evaluation of this term is discussed in the next section. The second integral in Eq. (1) induces a component of velocity as well. Note that this component alone need not equal that due to solid body rotation. This will be the case only for a circular cylinder. Therefore, the second integral must also be evaluated. It is convenient to evaluate this integral for the x and y components of velocity u_x and u_y. In this way, they combine directly with the prescribed translational velocity components of the body. Expressions for these will be presented in the next section.

Let P denote a given point on the body just interior to the surface, and let Q be any other point on the body surface. If one introduces the auxiliary bound vorticity function defined by $\hat{\gamma} \equiv \gamma h$, then the integral equation for $\hat{\gamma}$ is

$$\hat{\gamma}_P - \frac{(b/a)}{\pi}\int_0^{2\pi} K(\eta_P,\eta_Q)\hat{\gamma}_Q\,d\eta_Q = \frac{2}{c}\left[-(u_x - U_b)_P\sin\eta_P + \frac{b}{a}(u_y - V_b)_P\cos\eta_P - \frac{b}{a}\Omega\right] + 2\frac{h}{c}\left[(u_\eta)_{\text{outer}}\right]_P \tag{6}$$

where

$$K(\eta_P,\eta_Q)=\frac{1-\sin\eta_P\sin\eta_Q-\cos\eta_P\cos\eta_Q}{(\cos\eta_P-\cos\eta_Q)^2+(b^2/a^2)(\sin\eta_P-\sin\eta_Q)^2} \quad (7)$$

The bound vorticity γ_P corresponds to a velocity discontinuity across the body surface. Since Eq. (6) is derived from the requirement that the fluid interior to the body follow its prescribed motion, γ_P represents a local slip velocity component tangential to the body. This must be reduced to zero by the proper production of free vorticity at the body surface, thus providing the important coupling between the bound and free vorticity distributions.

Following the procedure of Ref. 5, the instantaneous vorticity production at any point of the body at time t produces a diffusive flow of vorticity from the body into the fluid. This is envisioned to take place over a suitably small time increment, Δt. Thus, one can write

$$\frac{1}{Re}\int_t^{t+\Delta t}\left(\frac{\partial\omega}{\partial\xi}\right)_{\xi_0}dt'=-\hat{\gamma}(t) \quad (8)$$

where it is important to keep in mind that $\hat{\gamma}$ is considered to be the known quantity, as determined from Eq. (6).

The solution to Eq. (6) is nonunique, since the homogeneous equation admits a complementary solution corresponding to pure circulatory flow about the body. This complementary solution for this geometry is simply a constant, say, $\hat{A}$. That is, $\hat{\gamma}=\hat{\gamma}_{\text{part}}+\hat{A}$. Where $\hat{\gamma}_{\text{part}}$ is the particular solution to the complete equation. The constant $\hat{A}$ must be evaluated from the global conservation of vorticity principle. This can be deduced in several ways. The procedure adopted here is based on a dynamical argument concerning the pressure field.

The dimensionless pressure gradient at the body surface is obtained from the tangential momentum equation. One obtains

$$\left(\frac{\partial P}{\partial\eta}\right)_{\xi_0}=\frac{1}{Re}\left(\frac{\partial\omega}{\partial\xi}\right)_{\xi_0}-\frac{b}{a}\frac{d\Omega}{dt}-\Omega^2c^2\sin\eta\cos\eta$$
$$+\left(\frac{dU_b}{dt}-\Omega V_b\right)\sin\eta-\frac{b}{a}\left(\frac{dV_b}{dt}+\Omega U_b\right)\cos\eta \quad (9)$$

where the pressure has been rendered nondimensional by $\rho\hat{U}^2$. Note that the fluid at the surface adheres to the body and, thus, has a nonzero absolute velocity. These inertia terms are included in Eq. (9). The integral of Eq. (9) with respect to η from 0 to 2π must yield zero if the pressure distribution is to be single valued. That is,

$$0=\frac{1}{Re}\int_0^{2\pi}\left(\frac{\partial\omega}{\partial\xi}\right)_{\xi_0}d\eta-2\pi\frac{b}{a}\frac{d\Omega}{dt} \quad (10)$$

which is the required statement of global conservation of vorticity for this problem. It differs from that derived in Ref. 5 by the second term on the right-hand side.

The next step is to combine Eqs. (8) and (10). Thus, Eq. (8) is integrated with respect to η from 0 to 2π, and Eq. (10) is integrated with respect to time from t to $t+\Delta t$. After equating like terms, one obtains

$$\int_0^{2\pi}\hat{\gamma}(\eta,t)\,d\eta=-2\pi\frac{b}{a}[\Omega(t+\Delta t)-\Omega(t)] \quad (11)$$

In contrast to the result employed in Ref. 5, the right-hand side of Eq. (11) is not zero if the body has a changing angular velocity.

Since the right-hand side of Eq. (11) is known, this equation provides the closure for the determination of $\hat{\gamma}$. It has a very simple interpretation. It states that the free vorticity given off to the fluid in time Δt must be equal and opposite to the vorticity gained by the interior replacement fluid during the same time increment. If the body has zero angular acceleration, then the right-hand side of Eq. (11) is identically zero.

Upon substituting $\hat{\gamma}=\hat{\gamma}_{\text{part}}+\hat{A}$ into the left-hand side of Eq. (11) and integrating, a final expression for $\hat{A}$ can be obtained. The complete solution for $\hat{\gamma}$ then becomes

$$\hat{\gamma}=\hat{\gamma}_{\text{part}}-\frac{1}{2\pi}\int_0^{2\pi}\hat{\gamma}_{\text{part}}\,d\eta-\frac{b}{a}[\Omega(t+\Delta t)-\Omega(t)] \quad (12)$$

Note that the term in brackets gives the total change in Ω in time Δt. This is a consequence of the expression used in Eq. (8). Implicit is the assumption that Δt is small. It is the time required for vorticity to diffuse from the surface into the first stratum of adjacent fluid.

In principle, the flow is completely specified by the given governing equations. Once these are solved, the surface forces acting on the body and the force coefficients can be determined.

The drag and lift forces per unit span are made nondimensional by $4\rho\hat{U}^2a$. They are, respectively, considered to act parallel and perpendicular to the instantaneous velocity vector of the body. This vector makes an angle α with the x axis, where $\alpha=\arctan V_b/U_b$, see Fig. 1. The moment per unit span is calculated about the origin and is made nondimensional by $4\rho\hat{U}^2a^2$. One has for these force coefficients

$$(C_D)_F=\frac{1}{Re}\left[\cos\alpha\int_0^{2\pi}\omega_{\xi_0}\sin\eta\,d\eta-\frac{b}{a}\sin\alpha\int_0^{2\pi}\omega_{\xi_0}\cos\eta\,d\eta\right] \quad (13a)$$

$$(C_D)_P=-\frac{b}{a}\frac{\cos\alpha}{Re}\int_0^{2\pi}\left(\frac{\partial\omega}{\partial\xi}\right)_{\xi_0}\sin\eta\,d\eta$$
$$+\frac{\sin\alpha}{Re}\int_0^{2\pi}\left(\frac{\partial\omega}{\partial\xi}\right)_{\xi_0}\cos\eta\,d\eta-\frac{\pi b}{a}[\dot{U}_b-\Omega V_b)\cos\alpha$$
$$+(\dot{V}_b+\Omega U_b)\sin\alpha] \quad (13b)$$

$$(C_L)_F=\frac{1}{Re}\left[\sin\alpha\int_0^{2\pi}\omega_{\xi_0}\sin\eta\,d\eta+\frac{b}{a}\cos\alpha\int_0^{2\pi}\omega_{\xi_0}\cos\eta d\eta\right] \quad (14a)$$

$$(C_L)_P=-\frac{b}{a}\frac{\sin\alpha}{Re}\int_0^{2\pi}\left(\frac{\partial\omega}{\partial\xi}\right)_{\xi_0}\sin\eta d\eta$$
$$-\frac{\cos\alpha}{Re}\int_0^{2\pi}\left(\frac{\partial\omega}{\partial\xi}\right)_{\xi_0}\cos\eta d\eta-\frac{\pi b}{a}[(\dot{U}_b-\Omega V_b)\sin\alpha$$
$$-(\dot{V}_b+\Omega U_b)\cos\alpha] \quad (14b)$$

$$(C_M)_F=\frac{(b/a)}{Re}\int_0^{2\pi}\omega_{\xi_0}d\eta-\frac{4\pi(b/a)}{Re}\Omega \quad (15a)$$

$$(C_M)_P=\frac{c^2}{2Re}\int_0^{2\pi}\left(\frac{\partial\omega}{\partial\xi}\right)_{\xi_0}\sin^2\eta d\eta-\frac{\pi c^2(b/a)}{2}\dot{\Omega} \quad (15b)$$

where the contributions due to the frictional shear stress and pressure have been given separately. Also note that the rectilinear accelerations are included for completeness.

All of the equations in this section can be specialized to the polar coordinate system. This is achieved formally by letting ξ become sufficiently large (say, >5) that $h\cong c\cosh\xi\cong c\sinh\xi=r$. Then $a=b$, and c approaches zero. Finally, $\partial/\partial\xi=r\,\partial/\partial r$, and η becomes the polar angle θ.

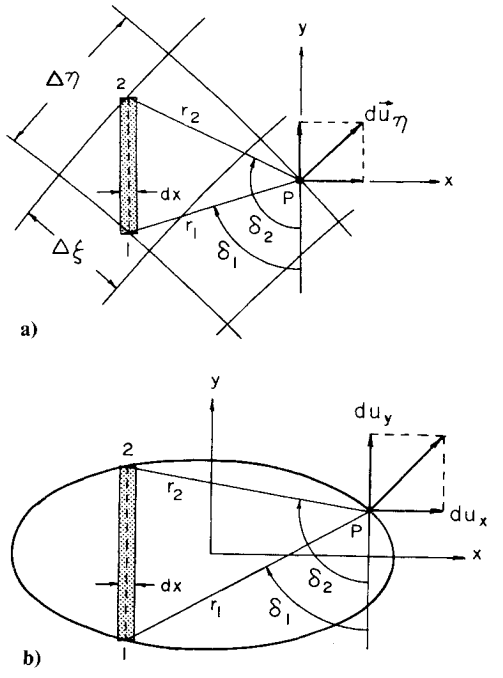

Fig. 2 Schematic diagram used in numerical evaluation of velocities induced by a) free and b) body vorticity.

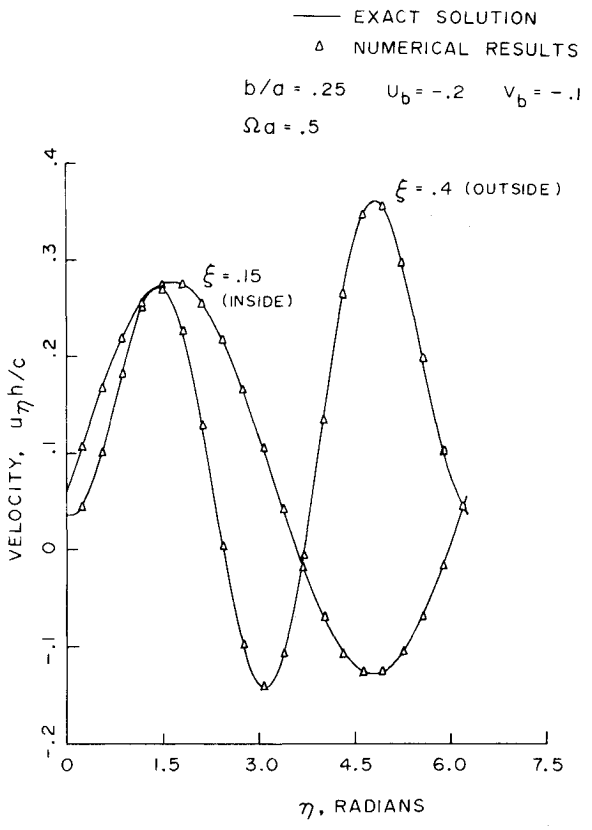

Fig. 3 Comparison of exact and numerical results for absolute velocity in η direction at locations inside and outside the rotating and translating elliptic cylinder for potential flow.

Numerical Formulation

The external flow is covered by a grid comprising 3200 control volumes. The periphery of the body is divided into increments of size $\Delta\eta = 2\pi/80$. The 80 points at which the bound vorticity is evaluated are centered in each interval $\Delta\eta$. There are 40 layers of control volumes extending laterally into the fluid. The increment $\Delta\xi$ is held constant at a value which depends on the particular flow to be analyzed. Specific choices will be given later.

Equations (2) and (5) are approximated using finite differences. The two-time-level explicit method is used to represent the temporal variation in Eq. (2). This, plus upwind convection and centrally differenced diffusion terms, follows the same procedures used in an earlier work.[3] In this regard, it is important to note that the velocity components in the η and ξ directions are evaluated centrally at the faces of each control volume. A node point is placed at the center of each control volume, and it is at this point that the vorticity is assigned its value.

The determination of the η component of velocity follows from a numerical evaluation of the terms in Eq. (1). These will be taken up separately.

Consider, first, the velocity induced by a differential strip element of free vorticity contained within a control volume $\Delta\eta\Delta\xi$. This is shown in Fig. 2a. From elementary kinematics, it can be shown that the strip induces velocity components du_x and du_y in a local Cartesian system as given by

$$du_x = -\left[\frac{\omega_f}{2\pi}\ell n\left(\frac{r_1}{r_2}\right)dx\right]\hat{i} \tag{16}$$

$$du_y = \left[\frac{\omega_f}{2\pi}(\delta_2 - \delta_1)\,dx\right]\hat{j} \tag{17}$$

The scalar component du_η is then

$$du_\eta = [du_x + du_y]\cdot\hat{e}_\eta \tag{18}$$

where

$$\hat{e}_\eta = (\sinh^2\xi + \sin^2\eta)^{-1/2}\,[-\cosh\xi\,\sin\eta\hat{i} + \sinh\xi\,\cos\eta\hat{j}] \tag{19}$$

Each control volume is divided into 40 elemental strips of varying but finite width. The radii r_1 and r_2 plus angles δ_1 and δ_2 are determined for each strip. The integration of du_η over the control volume is performed using 40-point Gauss-Legendre quadrature. The free vorticity ω_f is assumed to be constant over the control volume. If the point P is sufficiently far removed from the control volume, the free vorticity is approximated by a line vortex of strength $\omega_f\Delta\eta\Delta\xi$ concentrated at the centroid of the volume. This is done if the distance from the centroid to P is greater than $6\cdot(\Delta\eta\cdot\Delta\xi)^{1/2}$.

The evaluation of the second integral in Eq. (1) involving the body vorticity follows a similar procedure to that just described, except that 40-point Gauss-Legendre quadrature is used exclusively. The same procedure is valid whether or not the point P lies exterior or interior to the cylinder. If it lies interior (or on the surface), a line is projected through P which is perpendicular to the major axis. Each region within the ellipse to the right and left of the line is divided into 40 strip elements. The Cartesian components of the velocity induced by each strip are determined, as in Eqs. (16) and (17). Even for P inside the cylinder, the contribution due to each strip is bounded, so that the integral is not singular. This is because the width of each strip is finite. The results have been tested for conditions where the exact solution is known. This will be discussed later. The agreement between exact and numerical results is excellent. The final expressions for u_x and u_y are given as

$$(u_x)_P = -\frac{\Omega}{\pi}\int_{-1}^{+1}\ell n\left[\frac{(x_P-x)^2+(y_P-y_1)^2}{(x_P-x)^2+(y_P-y_2)^2}\right]^{1/2}dx \tag{20}$$

$$(u_y)_P = \frac{\Omega}{\pi}\int_{-1}^{+1}\left[\tan^{-1}\left(\frac{x_P-x}{y_P-y_2}\right)-\tan^{-1}\left(\frac{x_P-x}{y_P-y_i}\right)\right]dx \tag{21}$$

The quantities y_1 and y_2 in Eqs. (20) and (21) are defined in Fig. 2b, and these equations follow from Eqs. (16) and (17).

The final integral in Eq. (1) involves the bound vorticity of the surface. As mentioned earlier, the surface is initially covered by 80 points spaced at the center of equal intervals, $\Delta\eta$. The bound vorticity is determined directly at these 80 points. Four additional surface points are placed equally spaced in the η direction between pairs of original points. The bound vorticity at these intermediate points is found by linear interpolation. Finally, each surface segment is assumed to have vorticity of constant strength $\hat{\gamma}\Delta\eta$. Thus, one can write

$$\frac{1}{2\pi}\int_0^{2\pi}\frac{\hat{\gamma}_Q \hat{k}\times\mathbf{r}_{QP}}{r_{QP}^2}\,d\eta = \frac{1}{2\pi}\sum_{i=1}^{400}\left[\frac{(\cos\eta_P-\cos\eta_i)\hat{j}-(b/a)(\sin\eta_P-\cos\eta_i)\hat{i}}{(\cos\eta_P-\cos\eta_i)^2+(b^2/a^2)(\sin\eta_P-\cos\eta_i)^2}\right]\times\hat{\gamma}_i\Delta\eta_i \tag{22}$$

Finally, the component of this vector expression along the η direction is obtained by forming the scalar product of it with $\hat{e}_\eta$.

To summarize, at any field point P in the fluid, the induced velocity component in the η direction is comprised of a single contribution from the body vorticity, 80 contributions from the individual bound vorticity values, and 3200 contributions from the outer free vorticity values. Each contribution is given by a coefficient, which is only a function of the geometry, multiplied by a vorticity strength. The geometrical coefficients for all the field points were computed once and stored on magnetic tape. Spatial symmetry was used to reduce the number of evaluations. The coefficients were then retrieved whenever needed during the calculations.

Having thus evaluated u_η, the other component u_ξ is evaluated from a numerical analog of Eq. (5). This is

$$u_\xi\left(N\Delta\xi,\eta+\frac{\Delta\eta}{2}\right)=\frac{h(\xi_0,\eta+\Delta\eta/2)}{h(N\Delta\xi,\eta+\Delta\eta/2)}u_\xi\left(\xi_0,\eta+\frac{\Delta\eta}{2}\right)-\frac{\Delta\xi}{h(N\Delta\xi,\eta+\Delta\eta/2)}\sum_{i=1}^{N}\{[hu_\eta]_{\xi_i,\eta+\Delta\eta}-[hu_\eta]_{\xi_i,\eta}\} \tag{23}$$

The numerical evaluation of the bound vorticity distribution from Eq. (6) follows in a straightforward manner. The right-hand side of Eq. (6) is evaluated at each of the 80 surface points. The quantities u_x and u_y have been given in Eqs. (20) and (21). The quantity $(u_\eta)_{\text{outer}}$ is obtained by integrating du_η, as discussed in connection with the development leading to Eq. (18), except that P lies on the surface.

With the right-hand side of Eq. (6) known, the integral on the left-hand side is replaced by a sum over the 80 descrete bound vortex points on the surface, each having strength $\gamma_Q\Delta\eta_Q$. The kernel given by Eq. (7) is evaluated for each pair of points P and Q. However, some care has to be exercised in evaluating this kernel when P and Q are coincident, since the kernel becomes indeterminant. Its limiting value can be found by applying L'Hopital's rule twice. One obtains

$$\lim_{P\to Q}K(\eta_P,\eta_Q)=\frac{b/a}{2\pi(\sin^2\eta_P)+(b^2/a^2)(\cos\eta_P)} \tag{24}$$

When P is allowed to move to each of 80 surface points, there results a set of 80 linear simultaneous equations for the bound vorticity.

For the calculation of the force coefficients, the vorticity and its derivative, $\partial\omega/\partial\xi$, are needed at the wall. For the latter quantity, the result from Eq. (8) was used. That is, $(\partial\omega/\partial\xi)_{\xi_0}=-Re\hat{\gamma}/\Delta t$. The wall values for the vorticity were obtained from the computed velocity profiles. At the wall, $\omega_{\xi_0}=2\Omega+h_0^{-2}[\partial/\partial\xi(h\cdot q_\eta)]_{\xi_0}$. A second-degree curve was fitted to the product $h\cdot q$, using a point on the body and two in the adjacent fluid. The resulting expression is $\omega_{\xi_0}=2\Omega+[9(h\cdot q_\eta)_1-(h\cdot q_\eta)_2]/(3\Delta\xi h_0^2)$.

Computational Procedures

The computations are started at $t=0^+$ from an initial state of rest. The motion of the body is initiated, and the solution is advanced forward in time. In effect, the body is given a series of impulsive changes in angular and/or translational velocity. Thus, it is as straightforward to simulate a single large impulsive acceleration as a series of small step-wise variations in velocity. The diffusion of newly created free vorticity from the surface into the fluid always follows after the impulsive changes in body velocity.

Since the fluid vorticity is initially zero, the diffusive flux of free vorticity from the surface into the fluid is the only relevant term needed to advance the vorticity solution over the first time step using Eq. (2). This initial diffusive flux is given by Eq. (8) for $t=0^+$.

Thus, one begins with the solution for $\hat{\gamma}$ from Eq. (6) at $t=0^+$. For the case of zero vorticity in the fluid, $(u_\eta)_{\text{outer}}=0$ at every point on the cylinder surface. The other velocity components on the right-hand side of Eq. (6), including Ω, are assigned their values corresponding to $t=\Delta t$, but these are assumed to be attained instantaneously at $t=0^+$ and to remain constant over the time increment. Consequently, the entire nonhomogeneous term of Eq. (6) is known. Upon obtaining a particular solution to Eq. (6), the general solution is given by Eq. (12), where the term in brackets is $\Omega(\Delta t)$, since $\Omega(0)=0$. To finish the initial sequence, Eq. (2) is integrated forward in time subject to the diffusive flux boundary condition at the body surface, as given by Eq. (8).

At the beginning of the second complete loop through the calculations, there is a distribution of free vorticity in the fluid, which arose in the first sequence. This must now be used to evaluate $(u_\eta)_{\text{outer}}$ for input to Eq. (6). The remaining variables on the right-hand side of Eq. (6) are assigned their values at $2\Delta t$, and the solution for $\hat{\gamma}$ is obtained. With this, plus the known free and body vorticities, the velocity field in the fluid adjacent to the body is computed from Eqs. (1) and (5). The diffusive flux of free vorticity at the wall is also known from Eq. (8), where $t=\Delta t$. Thus, the vorticity transport equation, Eq. (2), is integrated over the second time increment. This completes the sequence. The subsequent calculations are repeated as just described, and so on and so forth.

Results and Discussion

The results from the numerical calculations have been compared with those of exact analyses wherever possible. In particular, Eq. (6) can be solved exactly for the case where $(u_\eta)_{\text{outer}}$ is identically zero. Also, exact expressions for the velocity components u_ξ and u_η for potential flow may be found using results in Lamb.[9] Detailed comparisons of the exact and numerically calculated values are given in graphical and tabular form in Ref. 8 for a variety of elliptic cylinders in combinations of pure translational and rotational motion. Only a sample is given here.

In Fig. 3, results for $u_\eta h/c$ are shown for locations inside and outside the elliptic cylinder. The aspect ratio b/a is 0.25, and the cylinder is moving in translation and rotation. The outer flow is assumed to be inviscid.

The triangular points are computed numerically for 20 locations equally spaced around each elliptical contour given

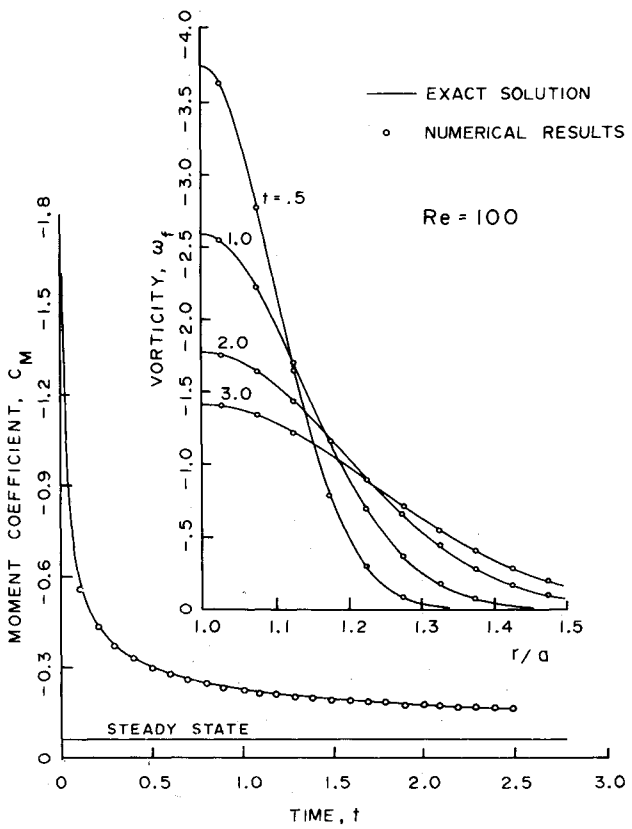

Fig. 4 Comparison of exact and numerical results for viscous flow outside a circular cylinder in pure rotation started impulsively from rest, $Re = 100$.

by $\xi = \text{const}$. The theoretical value for $u_\eta h/c$ is given by

$$u_\eta \frac{h}{c} = \frac{\Omega a}{c}\left[\frac{b}{a} - \frac{1}{2}\left(1+\frac{b}{a}\right)^2 e^{-2\xi}\cos 2\eta\right] + \frac{e^{\xi}\left[U_b (b/a)\sin\eta - V_b \sin\eta\right]}{1 - b/a} \tag{25}$$

for points outside the cylinder, and

$$u_\eta \frac{h}{c} = \Omega a\left(1-\frac{b^2}{a^2}\right)^{1/2} \sinh\xi\cosh\xi - U_b \cosh\xi\sin\eta + V_b \sinh\xi\cos\eta \tag{26}$$

for points inside the cylinder. Here the reference velocity $\hat{U}$ is taken to be $2\Omega^* a$, so that Ωa in Eqs. (25) and (26) equals 1/2. The agreement between exact and numerical results is generally to five significant figures.

The viscous-flow equations for the case of a circular cylinder in pure rotation about its axis can also be solved exactly, as shown by Mallick.[10] Since the problem is linear, any arbitrary time variation of the angular velocity may be treated using the principle of superposition, once the solution for a unit impulsive change in angular velocity is known. Results for a single unit impulsive acceleration, as well as a rotational velocity which varies exponentially with time, have been obtained numerically in Ref. 8. A representative comparison is given in Fig. 4 for a single impulsive angular acceleration. The reference velocity is again $2\Omega^* a$. The dimensionless time and spatial increments are given by $\Delta t = 0.01$ and $\Delta r = 0.05$, and $Re = 2\Omega^* a^2/\nu = 100$. The direction of rotation is counterclockwise, and the moment due to the fluid acting on the cylinder is clockwise (taken to be negative). The agreement between exact and numerical results is judged to be excellent.

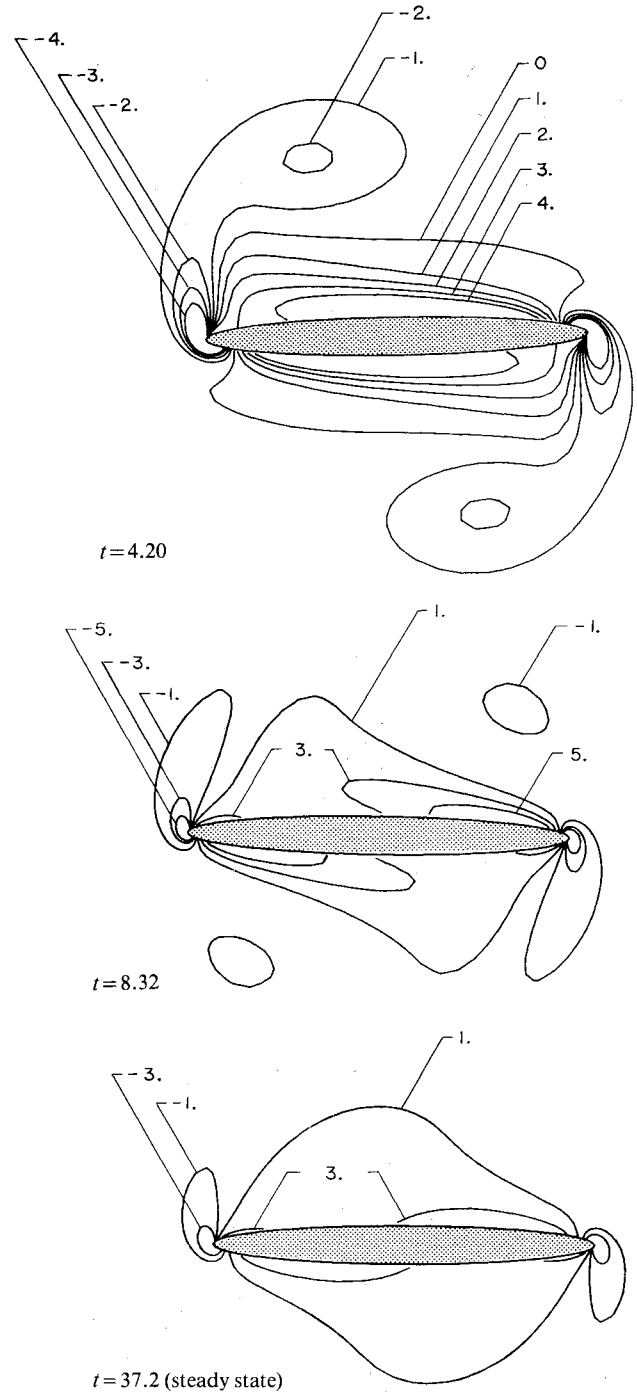

Fig. 5 Vorticity contours around an elliptic cylinder in pure rotation, $Re = 200$.

The present analysis has also been applied to two different flow configurations for which exact solutions are not known. These are described in the following sections.

Case A: Elliptic Cylinder in Pure Rotation

An elliptic cylinder is impulsively set into rotary motion from rest and is maintained at constant angular velocity Ω thereafter. The axis of rotation is about the centroid. The reference velocity is $\hat{U} = 2a\Omega^*$, the Reynolds number is $\hat{U}a/\nu = 200$, and the aspect ratio is $b/a = 0.0996$. This is identical to one of the problems analyzed previously by Lugt and Ohring,[11] when allowance is made for the different

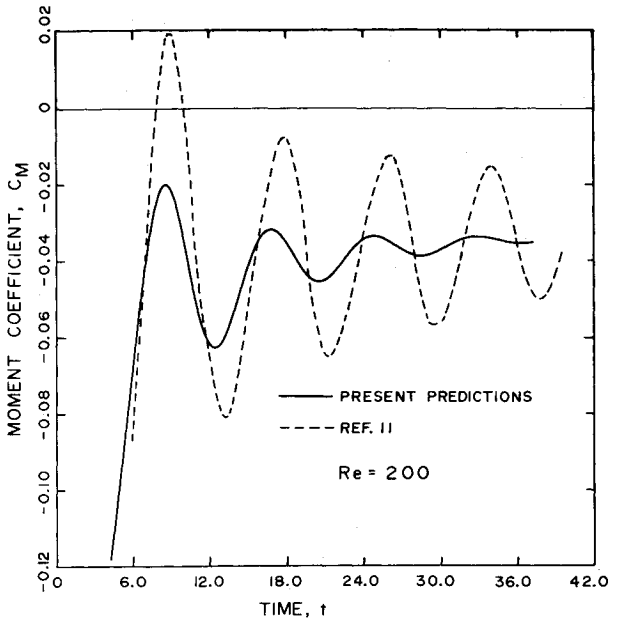

Fig. 6 Comparison of predictions for the moment coefficient for an elliptic cylinder in pure rotation, $Re = 200$.

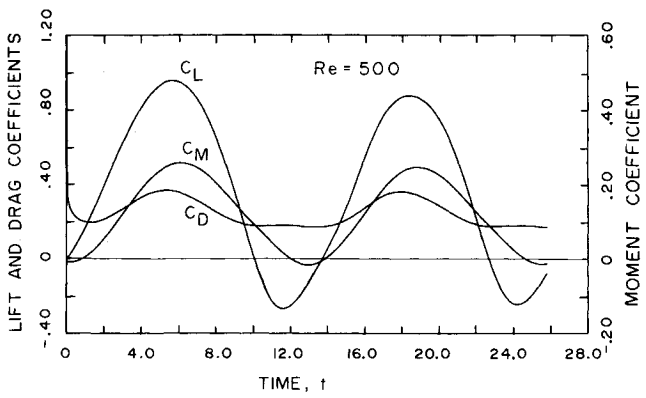

Fig. 7 Predicted force coefficients for a translating elliptic cylinder in pitching oscillation, $Re = 500$.

schemes used to nondimensionalize the variables. For these present calculations, $\Delta\eta = 2\pi/80$, $\Delta\xi = 0.04$, and Δt varies from 0.002 to 0.003. These are comparable to the values chosen in Ref. 11, which are $\Delta\eta = 2\pi/96$, $\Delta\xi = 0.04$, and $\Delta t = 0.0037$. Calculations were performed on a Control Data Corporation CYBER-175 and a UNIVAC 1110 in double precision.

Contours of constant vorticity are shown in Fig. 5 for three different times. These are selected to coincide with equivalent time values chosen by Lugt and Ohring.[11] Note, however, that the direction of rotation is reversed. Also, the present Reynolds number of 200 corresponds to their value of 400, and the present time values are twice theirs.

There is generally very good agreement between the vorticity contours of the present and earlier works. However, there are appreciable differences when one compares the predictions for the moment coefficient. A comparison of the present and earlier results is given in Fig. 6. In order to affect this comparison, the moment coefficient of Ref. 11 was divided by 8, and the sign was reversed. This was needed in order to account for the different sign convention and method of nondimensionalization. Of particular note is the difference in amplitude of oscillation. Those of Ref. 11 are much more pronounced. Indeed the moment changes sign during the first oscillation. This means that for a brief moment, the action of the fluid is to aid the rotation of the cylinder. Such behavior is not found in the present predictions, and the fluid always apposes the sense of rotation of the cylinder.

The moment coefficients appear to be approaching approximately the same steady-state limit, which is -0.034 in the present work and -0.030 (i.e., $-0.24/8$) in Ref. 11. Our predictions attain this limit in approximately one-half the time, however. The calculations in Ref. 11 are carried to a time of 13π, which is equivalent to 26π on the time axis of Fig. 6.

Reasons for the differences in the moment predictions can only be conjectured upon. It is noteworthy that both numerical approaches agree with the exact moment predictions for the case of a circular cylinder rotated impulsively. However, for this case, there is no pressure contribution to the moment, and there is axial symmetry to the flow. For a rotating elliptic body, approximately all of the moment is due to pressure forces. Therefore, it is important that the dynamics be properly modeled, even during the impulsive start. At the time of this first impulse, sufficient net vorticity must be imparted to the fluid to counter the total "residual vorticity" represented by the body, which is $\pi ab(2\Omega^*)$. The present approach guarantees this precise measure of vorticity production, as can be seen by the application of Eq. (11). At time $t = 0^+$, the angular velocity is zero. After one time step, the angular velocity is equal to that prescribed, and the right-hand side of Eq. (11) becomes $-\pi(b/a)\dot{\Omega}$, which is the proper measure of vorticity production in nondimensional terms. For all times thereafter, the net vorticity production (i.e., the total integrated amount over the surface) is zero, and this initially produced vorticity spreads throughout the fluid. It does not appear that the approach of Ref. 11 can account for this precise aspect of the vorticity dynamics. Since this initial amount of total negative vorticity is always present in the flow, its effect is permanent, although its importance would be expected to diminish with time. Perhaps this is why the steady-state moment coefficients show satisfactory agreement.

Case B: Elliptic Cylinder in Combined Translation and Rotation

An elliptic cylinder is impulsively set into translational motion with velocity $\hat{U}$. The translational velocity vector is constant and horizontal in an inertial reference frame. There is simultaneous pitching motion about the centroid. The pitching motion is harmonic, and the instantaneous angle of pitch from the horizontal axis is given by $\beta(t) = \pi/18\,(1 - \cos 0.5t)$. Referring to Fig. 1, one has $U_b = \cos\beta$, $V_b = \sin\beta$, and $\Omega = (\pi/36)\sin 0.5t$. The Reynolds number is 500, and $b/a = 0.25$. Here $\Delta\xi = 0.05$ and Δt varies between 0.011 and 0.02. Calculations were performed on the CRAY-1 computer of the NASA Ames Research Center.

No previously published results for this case are known to the authors. We emphasize here only the force predictions. The maximum angle of pitch is 20 deg, which is attained at $t = 2\pi$. Calculations have been carried out for two complete cycles. The results are shown in Fig. 7.

Note that the moment coefficient is initially slightly negative, but as soon as a small angle of attack is produced, the moment becomes positive and remains so until the cylinder returns to a horizontal position. The lift coefficient achieves its maximum at approximately $t = 6.0$, which is ahead of the maximum angle of attack. As the cylinder pitches downward, the lift continues to decrease and even goes negative, although the angle of attack is never less than zero. This behavior in lift is similar to that observed in Ref. 3 for a Joukowski airfoil held stationary in a flow with time-varying angle of attack. The elliptic cylinder, with its rounded leading and trailing edges, does not approximate the airfoil with a sharp trailing edge; nor are the surface dynamics the same. Therefore, the reasons for this similar behavior may be entirely different.

As the elliptic cylinder pitches up, the angular acceleration $\dot{\Omega}$ is positive until the angle of attack reaches 10 deg.

Therefore, over this portion of the cycle, there is a net negative production of free vorticity at the surface [see Eq. (11)]. As the angle increases from 10 to 20 deg, the net vorticity production becomes increasingly positive. At the maximum angle $\Omega = 0$, and the total net vorticity cast off from the surface into the fluid over this part of the cycle is zero. As the pitch angle decreases, positive vorticity is produced at the surface until the angle becomes 10 deg, after which negative net vorticity comes into production. It can thus be seen that only when the pitch angle is 0 and 20 deg is the total net vorticity in the boundary layer and wake zero. At all other times, it is nonzero. In contrast, a cylinder at rest in a flow with time-varying angle of attack has zero net vorticity production over the surface for all time. Therefore, the net vorticity of the wake is always zero.

Due to the dynamical dissimilarities already discussed, there is no direct analogy between the flow produced by a fixed object in a fluid with time-varying flow angle and that produced by an object which has an angular acceleration in an otherwise stationary fluid. The distributions of vorticity production at the surface are different, as are the instantaneous distributions of free vorticity in the fluid.

It is believed that the brief periods of negative lift shown in Fig. 7 could be due to leading-edge separation, which causes regions of relatively quiescent fluid to remain near the top surface, while fluid is swept rapidly from the lower surface. The nonlinear effects are very pronounced, and in the length of time necessary for the cylinder to rotate from 0 to 20 deg, the cylinder has only proceeded π-chord lengths. This means that the reduced circular frequency based on the chord and translational velocity is 1.0, which is relatively large. Clearly, more needs to be learned about such flows before all of these effects can be fully understood. The intent here is to demonstrate that such flows can be handled by the present analysis and numerical formulation.

Concluding Remarks

The two-dimensional analysis of unsteady viscous flows about bodies in arbitrary motion has been developed from basic kinematical and dynamical principles. The basis for the approach can be traced to the remarks by Lighthill[12] and, also, the book by Batchelor.[13]

As in an earlier work,[5] the essential part of the analysis involves the unique determination of the bound vorticity distribution on the surface of the body. This is needed to evaluate the surface production of the free vorticity that enters the fluid. It is also the principal ingredient to the calculation of the surface pressure distribution and, thus, the most important contribution to the fluid forces acting on the body.

The removal of the ambiguity to the solution for the bound vorticity requires a knowledge of the angular acceleration of the body through the principle of the conservation of total vorticity. This has been presented for two-dimensional flows in its most general form, thus enlarging the class of flows which can be treated by this method. It constitutes the essential closure for the problem in the same way that the Kutta-Joukowski condition renders potential-flow solutions unique. To the author's knowledge, no other analyses have incorporated this single most important principle. It is the essential strength of the method.

The method has been applied to cylinders in pure rotation, and those with simultaneous rotation and translation. The intent has been to demonstrate the suitability of the approach for a class of body motions with rotation. The example of Case B is particularly important because the angular acceleration changes continuously. More comparisons with the results of other analyses and experiments are needed in order to establish the accuracy of the predictions. However, the evidence to date indicates that the method is both rigorous and accurate, and further applications are planned for the future.

Acknowledgments

The authors express their appreciation to the Computer Centers of The University of Arizona and the U.S. Military Academy for providing access to the CDC CYBER-175 and UNIVAC 1110, respectively. The NASA Ames Research Center provided access to the CRAY-1 computer through the Computational Fluid Dynamics Traineeship Program.

References

[1] Mehta, U. S., "Dynamic Stall of an Oscillating Airfoil," *AGARD Conference Proceedings,* Vol. 227, Sept. 1977, pp. 23.1-23.32.

[2] Wu, J. C., "A Numerical Study of Unsteady Viscous Flows Around Airfoils," *AGARD Conference Proceedings,* Vol. 227, Sept. 1977, pp. 24.1-24.18.

[3] Kinney, R. B., "Two-dimensional Viscous-Flow Past an Airfoil in an Unsteady Airstream," *AGARD Conference Proceedings,* Vol. 227, Sept. 1977, pp. 26.1-26.14.

[4] Lugt, H. G. and Haussling, H. J., "The Acceleration of Thin Cylindrical Bodies in a Viscous Fluid," *Journal of Applied Mechanics,* Vol. 45, March 1978, pp. 1-6.

[5] Kinney, R. B. and Cielak, Z. M., "Analysis of Unsteady Viscous Flow Past an Airfoil: Part I—Theoretical Development," *AIAA Journal,* Vol. 15, Dec. 1977, pp. 1714-1719.

[6] Glauert, H., "The Accelerated Motion of a Cylindrical Body Through a Fluid," *Technical Report of the Aeronautical Research Committee,* Rept. and Memo. No. 1215, Jan. 1929, pp. 118-127.

[7] Wu, J. C., "Numerical Boundary Conditions for Viscous Flow Problems," *AIAA Journal,* Vol. 14, Aug. 1976, pp. 1042-1049.

[8] Taslim, M. E., "Analysis of Two-Dimensional Viscous Flow Over an Elliptic Body in Unsteady Motion," Ph.D. Thesis, University of Arizona, Tucson, Ariz., 1981.

[9] Lamb, H., *Hydrodynamics,* Dover, New York, 1945, pp. 84-89, 232.

[10] Mallick, D. D., "Nonuniform Rotation of an Infinite Circular Cylinder in an Infinite Viscous Liquid," *Zeitschrift fuer Angewandte Mathematik und Mechanik,* Vol. 37, Sept.-Oct. 1957, pp. 385-392.

[11] Lugt, H. J. and Ohring, S., "Rotating Elliptic Cylinders in a Viscous Fluid at Rest or in a Parallel Stream," *Journal of Fluid Mechanics,* Vol. 79, Pt. 1, 1977, pp. 127-156.

[12] Lighthill, M. J. "Introduction. Boundary Layer Theory," *Laminar Boundary Layers,* edited by J. Rosenhead, Oxford University Press, New York, 1963, pp. 54-61.

[13] Batchelor, G. K., *An Introduction To Fluid Dynamics,* Cambridge University Press, New York, 1970, pp. 84-99, 266-282.